SECOND EUROPEAN CONFERENCE ON EARTHQUAKE ENGINEERING
AND SEISMOLOGY, ISTANBUL AUG. 25-29, 2014

AN ANALYTICAL METHOD FOR ACTIVE FAULT VERIFICATION OF BURIED STEEL PIPELINES WITH BENDS

Dimitris KARAMITROS[1], George BOUCKOVALAS[2] and Christos ZOUPANTIS[3]

ABSTRACT

Existing analytical methodologies for the strength verification of buried steel pipelines against large permanent ground displacements, such as active fault ruptures, apply only to straight pipelines, not taking into account bends existing in their route. To fill this gap in the relevant literature, a new methodology is proposed herein for the analytical computation of pipeline strains developing in the presence of bends with arbitrary geometry (bend angle and radius of curvature), located outside the near-fault high-curvature zone, but within the pipeline's unanchored length. Comparison with results from 3D non-linear finite element analyses indicates that the proposed methodology captures the basic mechanisms of pipeline response, with both quantitative and qualitative accuracy. Additional conclusions of practical interest for pipeline design are finally drawn from a joint review of the numerical and analytical predictions.

INTRODUCTION

Permanent ground displacements (PGDs) is probably one of the most critical loading conditions that need to be taken into account for the design of buried pipelines (e.g. ALA-ASCE, 2004, O'Rourke & Liu, 1999). In earthquake-prone areas, such displacements are mainly associated to the rupture of active faults, although they may also originate from more common geotechnical causes, such as slope failures, lateral spreading, etc. In that case, a rigorous computation of pipeline strains requires the use of numerical analyses which take consistently into account the 3D geometry of the pipeline axis, the non-linear response of the pipeline steel and the surrounding backfill material, as well as the pipeline-soil interaction. The complexity of such analyses may vary widely depending on the simulation of the pipeline and the surrounding soil. For instance, the pipeline may be simulated with finite beam or pipe elements (e.g. Odina et al. 2009, Joshi et al. 2011, Karamitros et al. 2011), or with more complex shell elements (e.g. Takada et al. 1998, Koumousis et al. 2002, Xie et al. 2011, Xie et al. 2013, Roudsari et al. 2013). On the other hand, the backfill can be simulated using distributed elstoplastic Winkler type springs (e.g. Koumousis et al. 2002, Odina et al. 2009, Gu & Zhang 2009, Arifin et al. 2010, Joshi et al. 2011, Xie et al. 2011), or as an elastoplastic discretized continuum (e.g. Daiyan et al. 2010, Roudsari et al. 2013, Xie et al. 2013).

In any case, the aforementioned numerical analyses require considerable expertise and they are time consuming, so that their application is usually restricted to the detailed design of large diameter thin-wall pipelines, which run the risk of crack development and/or buckling under the action of large PGDs. In many other occasions, engineers increasingly rely upon user-friendly analytical solutions, which allow parametric analyses to be performed at a fraction of the time required for a consistent

[1] Lecturer in Civil Engineering, University of Bristol, U.K., d.karamitros@bristol.ac.uk
[2] Professor, Geotechnical Department, National Technical University of Athens, Greece, gbouck@central.ntua.gr
[3] Civil Engineer, MSc, National Technical University of Athens, Greece, christos.zoupantis@gmail.com

numerical investigation (e.g. Karamitros et al, 2007, 2011, Trifonov & Cherniy, 2010, 2012). A common simplification of the analytical solutions is that the pipeline axis is considered straight for a large distance from the fault crossing. The only (known to the Authors) exception is the analytical solution proposed by O'Rourke & Liu (1999), which takes into account the existence of bends in the vicinity of the fault. Nevertheless, the range of application of this solution is limited by a number of over-simplifying assumptions, namely that it refers exclusively to 90° bends, it does not take into account the arch-shaped geometry of the bend, while the pipeline steel is assumed to behave elastically.

To this extent, the present study attempts to remedy the above limitations. More specifically, based on the elastic beam theory, an analytical solution is presented for the active fault verification of pipelines with curved bends, for a wide range of bend angles, curvature radii, bend to fault trace distances, as well as tensile displacements applied to the pipeline due to the ground rupture. A bilinear stress-strain relationship is considered for the pipeline steel, while the Winkler-type soil springs are taken as elastic-perfectly plastic. Following an analytical presentation of the basic modelling assumptions and the resulting equations, the accuracy of the analytical predictions is evaluated against the results of 3D numerical analyses with the Finite Element Method.

PROPOSED ANALYTICAL METHODOLOGY

Basic assumptions

The proposed methodology initially focuses upon the calculation of axial and bending strains in the zone of the pipeline bend (Step 1). This part of the pipeline is analysed using the direct stiffness method, as an arched elastic beam with an equivalent secant Young's modulus, in order to indirectly take into account the non-linear behaviour of pipeline steel. A basic requirement for the application of the proposed methodology is that the pipeline bend does not lie within the high-curvature zone, near the fault crossing, but within the pipeline's unanchored length. It should be noted, however, that the pipeline's curved length typically ranges from 20 to 50D, with D being the pipeline's diameter, while the unanchored length may exceed 200D on each side of the fault.

The pipeline's behaviour near the bend is derived as a function of the axial component of the applied fault displacement, by employing equations of displacement compatibility (Step 2). This procedure allows to calculate the axial force developing on the pipeline at the fault crossing. This force can be consequently implemented into any of the existing analytical methodologies for the strength verification of pipelines near fault crossings, allowing to quantify the effect of the pipeline's geometry on the strains developing at the fault crossing (Step 3).

Step 1: Analysis of the bend

The bent part of the pipeline is analysed as an arched elastic beam, with an axial displacement u_A being applied at its end A, as shown in Figure 1. A rotational and a transverse transitional spring are considered to support the beam at point A, while an axial and a transverse spring are considered at point B. The spring constants are computed in the following paragraphs. It should be noted that preliminary numerical analyses, such as the ones presented in the following Section, indicated that the bending moment developing at point B is very small, thus no rotational spring was considered at that end of the beam. Apart from the aforementioned supports, the beam is loaded with an axial uniformly distributed load t_u equal to the ultimate friction force applied by the surrounding soil, as well as a transverse load q_u, equal to the ultimate soil resistance for transverse pipeline displacement.

The beam is solved using the direct stiffness method. More specifically, the beam's equation of equilibrium is:

$$\{P\} - \{P_L\} = \left([K] + \left[K_{spr} \right] \right) \{u\} \quad (1)$$

where $\{P\}=\{F_A \quad Q_A \quad M_A \quad F_B \quad Q_B \quad M_B\}^T$ are the developing axial forces F, shear forces Q and bending moments M at the ends A and B of the beam, $\{P_L\}$ are the respective reaction forces

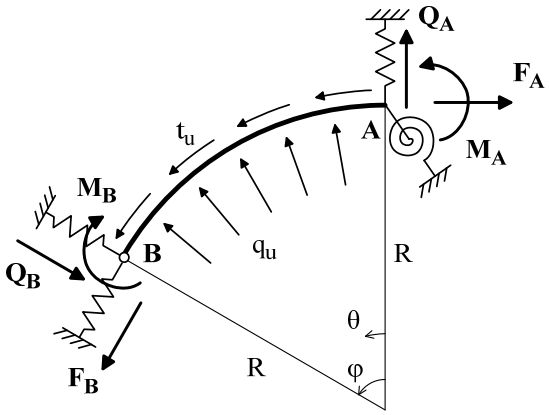

Figure 1. Model of the arched pipeline bend.

corresponding to loads t_u and q_u, $[K]$ is the stiffness matrix of the arched beam, $[K_{spr}]$ is the springs matrix and $\{u\}=\{u_A \quad v_A \quad \varphi_A \quad u_B \quad v_B \quad \varphi_B\}^T$ are the axial displacements u, the transverse displacements v and the rotations φ of the ends A and B of the beam.

Considering the beam's equilibrium without the external loads t_u and q_u, yields:

$$\{P_B\}=\begin{Bmatrix} F_B \\ Q_B \\ M_B \end{Bmatrix}=\begin{bmatrix} \cos\varphi & \sin\varphi & 0 \\ -\sin\varphi & \cos\varphi & 0 \\ R(\cos\varphi-1) & R\sin\varphi & 1 \end{bmatrix}\begin{Bmatrix} F_A \\ Q_A \\ M_A \end{Bmatrix}=[\Lambda]\{P_A\} \tag{2}$$

Therefore, the stiffness matrix $[K]$ can be calculated with the aid of the above transpose matrix $[\Lambda]$:

$$[K]=\begin{bmatrix} [F]^{-1} & \left([F]^{-1}\right)^T[\Lambda]^T \\ [\Lambda][F]^{-1} & [\Lambda]\left([F]^{-1}\right)^T[\Lambda]^T \end{bmatrix} \tag{3}$$

where $[F]$ is the flexibility matrix of an arched beam, similar to the one examined herein, but with a fixed support at point B and with no supports at point A. The elements of this flexibility matrix can be calculated using the principle of virtual works:

$$F_{ij}=\int_0^{\varphi}\frac{M_i(\theta)\cdot M_j(\theta)}{EI}Rd\theta \tag{4}$$

where $M_i(\theta)$ is the bending moment distribution along the beam AB, for an applied unit axial force (i=1), shear force (i=2) and moment (i=3) at point A. More specifically:

$$M_1(\theta)=R(\cos\theta-1) \tag{5a}$$

$$M_2(\theta)=R\sin\theta \tag{5b}$$

$$M_3(\theta)=1 \tag{5c}$$

Therefore:

$$[F]=\begin{bmatrix} \frac{R^3}{EI}\left(\frac{3\varphi}{2}+\frac{\sin 2\varphi}{4}-2\sin\varphi\right) & \frac{R^3}{EI}\left(\cos\varphi-\frac{\cos 2\varphi}{4}-\frac{3}{4}\right) & \frac{R^2}{EI}(\sin\varphi-\varphi) \\ & \frac{R^3}{EI}\left(\frac{\varphi}{2}-\frac{\sin 2\varphi}{4}\right) & \frac{R^2}{EI}(1-\cos\varphi) \\ & & \frac{R}{EI}\varphi \end{bmatrix} \tag{6}$$

Considering the same arched cantilever beam, with a fixed support at point B, the reactions to the applied soil friction forces t_u and the transverse soil resistance forces q_u may be calculated using equations of equilibrium:

$$\{P_{BL}\}=\begin{Bmatrix} F_{BL} \\ Q_{BL} \\ M_{BL} \end{Bmatrix}=\begin{Bmatrix} R\,q_u(1-\cos\varphi)-R\,t_u\sin\varphi \\ R\,q_u\sin\varphi+R\,t_u(1-\cos\varphi) \\ R^2\,t_u(\varphi-\sin\varphi)+R^2\,q_u(1-\cos\varphi) \end{Bmatrix} \tag{7}$$

The corresponding axial displacement (i=1), transverse displacement (i=2) and rotation (i=3) of point A may be calculated with the aid of the principle of virtual works:

$$\Delta_{AL,i}=\int_0^{\varphi}\frac{M_i(\theta)\cdot M_L(\theta)}{EI}Rd\theta \tag{8}$$

where M_L is the bending moment distribution developing due to the above loading:

$$M_L(\theta)=R^2\,t_u(\theta-\sin\theta)+R^2\,q_u(1-\cos\theta) \tag{9}$$

Therefore, the following matrix may be assembled:

$$\{\Delta_{AL}\}=\frac{R^3}{EI}\cdot\begin{Bmatrix} t_uR\left(\varphi\sin\varphi-\frac{\varphi^2}{2}-\frac{\sin^2\varphi}{2}\right)+q_uR\left(2\sin\varphi-\frac{\sin 2\varphi}{4}-\frac{3\varphi}{2}\right) \\ t_uR\left(\sin\varphi-\varphi\cos\varphi-\frac{\varphi}{2}+\frac{\sin 2\varphi}{4}\right)+q_uR\left(1-\cos\varphi-\frac{\sin^2\varphi}{2}\right) \\ t_u\left(\frac{\varphi^2}{2}+\cos\varphi-1\right)+q_u(\varphi-\sin\varphi) \end{Bmatrix} \tag{10}$$

Utilizing the above matrix, in combination with $[F]$ and $[\Lambda]$, the reaction matrix $\{P_L\}$ may be formed:

$$\{P_L\}=\begin{Bmatrix} [F]^{-1}\{\Delta_{AL}\} \\ [\Lambda][F]^{-1}\{\Delta_{AL}\}+\{P_{BL}\} \end{Bmatrix} \tag{11}$$

The opposite of this matrix is applied to the beam as a loading, as indicated by Equation 1.

The constants of the transverse and rotational springs that have been considered to support the ends A and B of the examined arched beam are calculated assuming that the pipeline away from the bend is behaving as a semi-infinite elastic beam on elastic foundation with a Winkler-type spring constant equal to k (Figure 2).

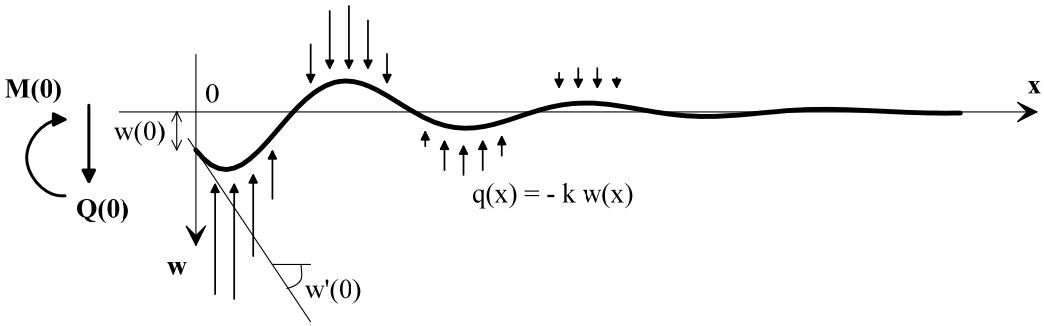

Figure 2. Model of semi-infinite elastic beam on elastic foundation.

Therefore, the elastic line w may be described by the following differential equation:

$$E_1 I \frac{d^4 w}{dx^4} + kw = 0 \tag{12}$$

Imposing into the above equation that $w \to 0$ when $x \to \infty$, yields:

$$w = e^{-\lambda x} C_1 \sin\lambda x + e^{-\lambda x} C_2 \cos\lambda x \tag{13a}$$

$$\text{where: } \lambda = \sqrt[4]{\frac{k}{4E_1 I}} \tag{13b}$$

Taking also into account that $M = -EI\frac{d^2 w}{dx^2}$ and $Q = EI\frac{d^3 w}{dx^3}$, the following boundary conditions may be derived:

$$Q(0) = 4EI\lambda^3 w(0) + 2EI\lambda^2 \frac{dw(0)}{dx} \tag{14a}$$

$$M(0) = 2EI\lambda \frac{dw(0)}{dx} + 2EI\lambda^2 w(0) \tag{14b}$$

Equations 14a and b essentially provide the spring constants for the supports of node A. For node B, there is no rotational spring, thus $M(0) = 0$. Therefore:

$$Q(0) = 2EI\lambda^3 w(0) \tag{15}$$

It should be noted that Equations 14a and b are coupled, thus the spring matrix contains non-zero elements outside the main diagonal.

As far as the axial spring at end B of the arched beam is concerned, its constant may be calculated by examining the axial stress and strain distribution in the straight part of the pipeline, away from the bend. More specifically, the axial force developing in this part of the pipeline is linearly decreasing with the distance from point B, due to the constant friction force t_u applied by the surrounding soil, until it becomes zero at a distance $L_{anch} = F_B / t_u$. The elongation of this part of the pipeline can be calculated by considering elastic behaviour for the pipeline steel and integrating the strains along its length:

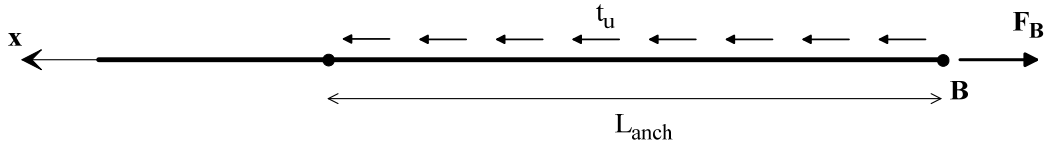

Figure 3. Straight pipeline model away from the bend.

$$u_B = \int_0^{L_{anch}} \varepsilon(x)dx = \int_0^{L_{anch}} \frac{F(x)}{E_1 A}dx = \int_0^{L_{anch}} \frac{F_B - t_u x}{E_1 A}dx = \frac{F_B^{\,2}}{2E_1 A t_u} \tag{16}$$

The constant for the axial spring at node B may be therefore calculated as follows:

$$k_{u,B} = \frac{dF_B}{du_B} = \frac{E_1 A t_u}{F_B} \tag{17}$$

It should be observed that the above constant is a function of the axial force at point B, which is not a priori known. Therefore, the analysis of the pipeline needs to be performed iteratively, until convergence is achieved.

According to the above, the spring matrix is constructed as follows:

$$[K_{springs}] = \begin{bmatrix} 0 & 0 & 0 & 0 & 0 & 0 \\ 0 & 4EI\lambda^3 & 2EI\lambda^2 & 0 & 0 & 0 \\ 0 & 2EI\lambda^2 & 2EI\lambda & 0 & 0 & 0 \\ 0 & 0 & 0 & EAt_u/F_B & 0 & 0 \\ 0 & 0 & 0 & 0 & 2EI\lambda^3 & 0 \\ 0 & 0 & 0 & 0 & 0 & 0 \end{bmatrix} \tag{18}$$

Finally, the following system of equations is derived:

$$\begin{Bmatrix} \{P_s\}_{1x1} \\ \{P_f\}_{5x1} \end{Bmatrix} = \begin{bmatrix} [K_{ss}]_{1x1} & [K_{sf}]_{1x5} \\ [K_{fs}]_{5x1} & [K_{ff}]_{5x5} \end{bmatrix} \begin{Bmatrix} \{u_s\}_{1x1} \\ \{u_f\}_{5x1} \end{Bmatrix} \tag{19}$$

The unknown quantities in Equation 19 are the axial force at node A $\{P_s\} = F_A$ and the displacements $\{u_f\} = \{v_A \quad \varphi_A \quad u_B \quad v_B \quad \varphi_B\}^T$, which are calculated according to the applied displacement $\{u_s\} = u_A$, as:

$$\{u_f\} = [K_{ff}]^{-1}\left(\{P_f\} - [K_{fs}]\{u_s\}\right) \tag{20}$$

$$\{P_s\} = [K_{ss}]\{u_s\} + [K_{sf}]\{u_f\} \tag{21}$$

The distribution of bending moments and axial forces can be consequently derived as:

$$M = M_A + Q_A R\sin\theta - F_A(R - R\cos\theta) + R^2 t_u(\varphi - \sin\theta) - R^2 q_u(\cos\theta - 1) \tag{22}$$

$$F = F_A\cos\theta + Q_A\sin\theta - Rq_u(\cos\theta - 1) - Rt_u\sin\theta \tag{23}$$

In the previously presented solution, the pipeline was considered to behave elastically. In order to account for the non-linear behaviour of the pipeline steel, the above procedure is repeated, using an equivalent secant Young's modulus E' for the pipeline steel, in order to achieve compatibility between the stresses and strains developing on the pipeline, at the position where the maximum bending moment M_{max} occurs. The exact distribution of stresses on the pipeline's cross-section is computed for this purpose, as a function of the developing bending and axial strains, ε_b and ε_a, respectively (Figure 4). The stress-strain relationship of the pipeline steel is considered to be bilinear, with initial Young's modulus E_1, yielding strain ε_1, and tangent Young's modulus after yield E_2.

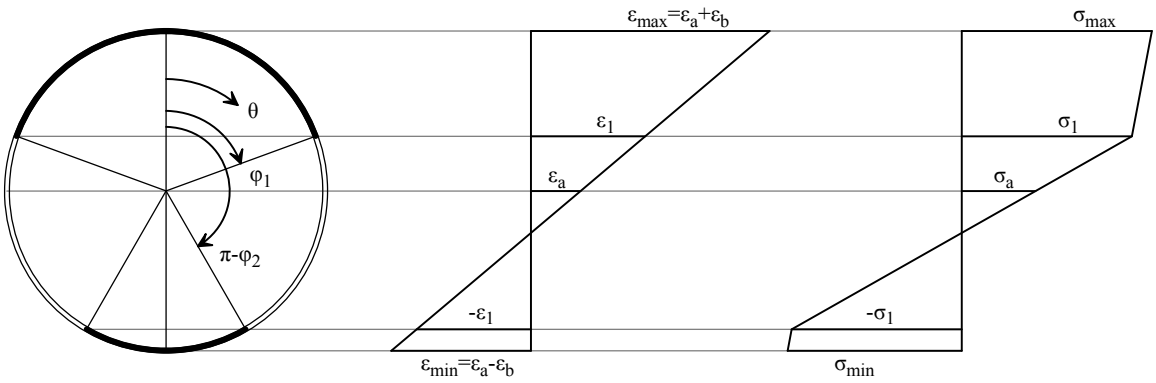

Figure 4. Non-linear strain and stress distribution over the pipeline's cross-section.

The bending strains are calculated as a function of the developing maximum bending moment:

$$\varepsilon_b = \frac{M_{max} D}{2EI} \tag{24}$$

while the corresponding axial strains ε_a are determined based on the requirement that the integral of stresses on the pipeline's cross-section is equal to the axial force F developing at the position where the maximum bending moment occurs. This condition is expressed as:

$$F = t(t-D)\begin{bmatrix} \varepsilon_a(\varphi_1+\varphi_2)(E_1-E_2) - \pi E_1 \varepsilon_a \\ +\varepsilon_b(E_1-E_2)(\sin\varphi_1 - \sin\varphi_2) \\ -\varepsilon_1(E_1-E_2)(\varphi_1-\varphi_2) \end{bmatrix} \tag{25}$$

$$\text{where } \varphi_{1,2} = \begin{cases} \pi & , \dfrac{\varepsilon_1 \mp \varepsilon_a}{\varepsilon_b} < -1 \\ \arccos\left(\dfrac{\varepsilon_1 \mp \varepsilon_a}{\varepsilon_b}\right) & , -1 \le \dfrac{\varepsilon_1 \mp \varepsilon_a}{\varepsilon_b} \le 1 \\ 0 & , \dfrac{\varepsilon_1 \mp \varepsilon_a}{\varepsilon_b} < 1 \end{cases} \tag{26}$$

Equation (25) can be solved iteratively with the Newton-Raphson method, as described by Karamitros et al (2007, 2011). Having calculated the stress distribution on the pipeline's cross-section, the associated bending moment may be computed as follows:

$$\begin{aligned} M = -\frac{t(t-D)^2}{2}\Bigg[& \frac{\varepsilon_b(\varphi_1+\varphi_2)(E_1-E_2)}{2} - \varepsilon_1(\sin\varphi_1+\sin\varphi_2)(E_1-E_2) \\ & -\frac{\pi E_1 \varepsilon_b}{2} + \varepsilon_a(E_1-E_2)(\sin\varphi_1 - \sin\varphi_2) + \frac{\varepsilon_b(E_1-E_2)(\sin 2\varphi_1 + \sin 2\varphi_2)}{4} \Bigg] \end{aligned} \tag{27}$$

The equivalent secant Young's modulus E' is consequently calculated based on the relationship between the bending strains ε_b and the corresponding bending moment M:

$$E' = \frac{MD}{2I\varepsilon_b} \tag{28}$$

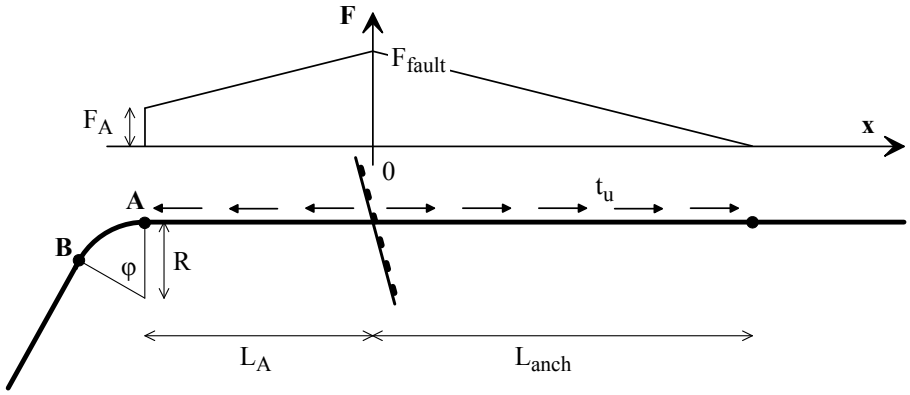

Figure 5. Pipeline axial force distribution.

The above procedure is then repeated, using the secant Young's modulus instead of the elastic one, until convergence is accomplished.

Step 2: Pipeline bend – fault crossing interaction

The interaction between the curved part of the pipeline and the fault crossing is quantified by considering the compatibility between the developing axial strains along the pipeline, the pipeline's elongation due to the axial component Δx of the applied fault displacement, as well as the displacement u_A of point A, at the bend. The distribution of axial strains is determined by considering an elastic stress-strain behaviour for the pipeline steel, as well as a linear distribution of axial forces along the pipeline, due to the constant value of the friction force t_u applied by the surrounding soil. More specifically, in the side of the bend, the axial force varies from F_A at point A of the bend, to $F_{fault} = F_A + t_u L_A$ at the fault crossing, while, in the other side, the axial force varies from F_{fault} at the fault crossing, to $F = 0$, at a distance $L_{anch} = F_{fault}/t_u$, as shown in Figure 5. According to the above:

$$\Delta x = u_A + \int_0^{L_A} \frac{F_A + t_u x}{EA} dx + \int_0^{L_{anch}} \frac{F_{fault} - t_u x}{EA} dx \Rightarrow u_A = \Delta x - \frac{2F_A L_A + t_u L_A^2 + F_A^2 / 2t_u}{EA} \qquad (29)$$

The axial force F_A in Equation 29 is not a priori known. Therefore, a value of $F_A = 0$ is initially considered, allowing for the estimation of an initial displacement u_A, which is subsequently applied to node A of the pipeline bend. The axial force F_A is then calculated from the first step of the methodology, the displacement u_A is consequently redefined using Equation 29 and the procedure is repeated until convergence is accomplished.

Step 3: Strength verification at the fault crossing

Having calculated the axial force F_A at point A of the pipeline's bend, the axial force F_{fault} at the fault crossing may also be calculated as described in Step 2. This force can be subsequently implemented into any of the existing methodologies for the strength verification of straight pipelines at fault crossings (e.g. Karamitros et al, 2007, Karamitros et al, 2012, Trivonov & Cherniy, 2011), allowing to quantify the effect of the bend on the strains developing in the near-fault high-curvature zone.

EVALUATION OF PROPOSED METHODOLOGY

The accuracy of the proposed methodology was evaluated through comparison with numerical predictions from parametric numerical analyses with the Finite Element code ANSYS 12. In more detail, numerical analyses were performed for a 0.9144m (36") diameter high pressure natural gas pipeline, with 0.0119m wall thickness, made of API5L-X65 carbon steel. The pipeline was discretized into 0.50m long elastoplastic beam elements, while the interaction with the backfill was simulated

with elastoplastic Winkler-type springs, defined according to ALA-ASCE (2005) guidelines for 1.30m thick cover of silica sand with friction angle φ=36º and dry unit weight γ=18KN/m^2. The pipeline route included a bend of angle φ, which varied parametrically from 0° (straight axis) to 90°, with a radius of curvature R, which similarly varied between 5D and 40D, where D is the nominal pipe diameter. The pipeline axis crossed the trace of a strike-slip fault at a crossing angle of 45° and a distance L_A from the bend, which varied parametrically from 50D to 200D. Permanent ground displacements of up to 2.0D were applied at the fixed end of the Winkler springs which overlay the sliding wall of the fault. Note that the parametric analyses were performed with reference to a basic case with L_A/D=100, φ=45° and R/D=10.

The results from the numerical analyses are compared against the analytical predictions in Figure 6, in terms of maximum pipeline strains developing at the bend, as well as in the vicinity of the fault crossing. Different graphs are used to show the effect of bend distance from the fault trace (L_A/D), the bend angle (φ), the bend radius (R/D) and the applied fault displacement (Δf/D). The agreement in all graphs is fairly consistent, indicating that the proposed methodology captures the basic mechanisms of pipeline response with both quantitative and qualitative accuracy.

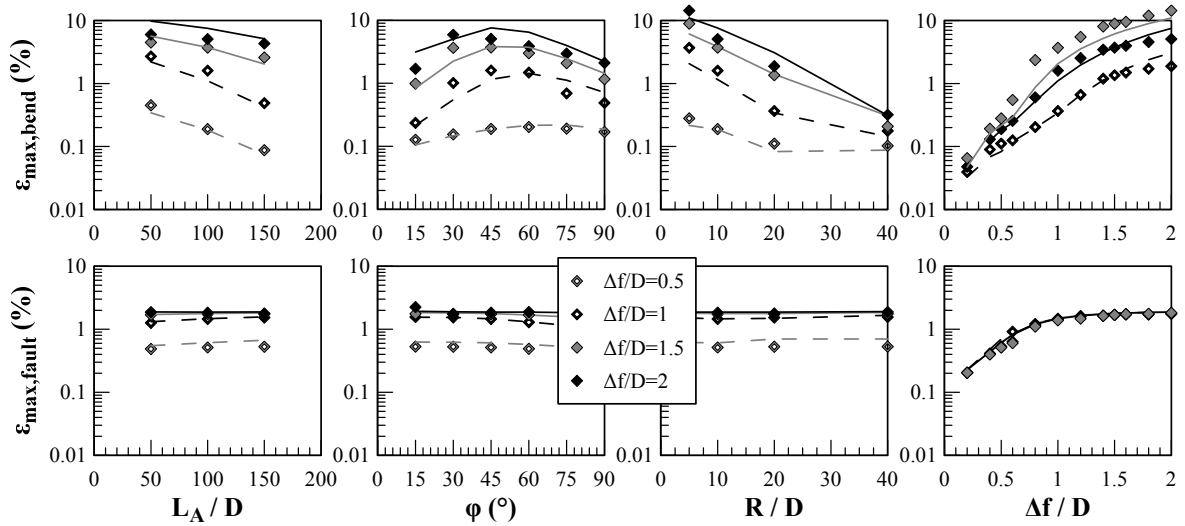

Figure 6. Comparison between numerical results (points) and analytical predictions (lines).

CONCLUDING REMARKS

The study presented herein focuses upon the strains developing in buried steel pipelines with bends, due to permanent ground displacements. Aiming to fill the gap in the existing literature, a new analytical methodology has been developed, which takes consistently into account the characteristics of the bend (angle φ and radius R), its distance from the fault trace (L_A), as well as the strength of the pipeline steel and the elastoplastic reaction of the surrounding soil.

Comparison with results from non-linear numerical analyses indicates that the proposed analytical methodology may provide a fairly accurate simulation of the pipeline response, at the critical sections around the bend, as well as at the vicinity of the fault crossing, so that it can be readily used for preliminary design purposes. Furthermore, the numerical and analytical predictions reviewed in this study (i.e. Figure 6) reveal some additional conclusions of practical interest for the pipeline design, namely that:

a. The effect of bends on pipeline strains at the fault trace is minor. Hence, pipeline strains at this region may be computed with methods developed for straight pipelines.
b. The most severe bend angle is not 90°, as suggested by O'Rourke & Liu (1999), but ranges between 30° and 45°.
c. As fault displacements increase and/or the distance of bends from the fault trace decreases, pipelines strains at the bend gradually exceed the strains at the fault trace, and

become critical for the pipeline design. The difference may reach an order of magnitude, for the above mentioned bend angles (30-45°) and small radii of curvature (R/D =5÷10).

d. Increasing the radius of curvature is an efficient way to reduce pipeline strains at the bends.

Finally, note that the present study is still in progress, aiming to further refine the analytical predictions for large applied displacements, small distances from the fault and small radii of curvature, as well as, to come up with solid guidelines and design recommendations.

ACKNOWLEDGEMENTS

This research has been co-financed by the European Union (European Social Fund – ESF) and Hellenic National Funds through the Operational Program "Education and Lifelong Learning" (NSRF 2007-2013) – Research Funding Program "Aristeia II".

REFERENCES

American Lifelines Alliance—ASCE (2005): "Guidelines for the Design of Buried Steel Pipe", July 2001 (with addenda through February 2005).

Arifin R.B., Shafrizal W.M., Wan B., Yusof M., Zhao P. & Bai Y. (2010), "Seismic analysis for the subsea pipeline system", Proceedings of the ASME 2010 29th interna- tional conference on ocean, offshore and arctic engineering, OMAE2010-20671, Shanghai, China.

Daiyan N., Kenny S., Phillips R. & Popescu R. (2010), "Numerical investigation of oblique pipeline/soil interaction in sand", Proceedings of the 8th international pipeline conference, IPC2010-31644. Calgary, Alberta, Canada.

Gu X. & Zhang H. (2009), "Research on a-seismatic measures of gas pipeline crossing a fault for strain-based design", Proceedings of the ASME 2009 pressure vessels and piping division conference, PVP2009-77987.

Joshi S., Prashant A., Deb A. & Jain S.K. (2011), "Analysis of buried pipelines subjected to reverse fault motion", Soil Dynamics and Earthquake Engineering 31, pp. 930–940.

Karamitros, D.K., Bouckovalas, G.D., Kouretzis, G.P. (2007): "Stress analysis of buried steel pipelines at strike-slip fault crossings", Soil Dynamics and Earthquake Engineering, 27 (3), pp. 200-211.

Karamitros, D.K., Bouckovalas, G.D., Kouretzis, G.P., Gkesouli, V. (2011): "An analytical method for strength verification of buried steel pipelines at normal fault crossings", Soil Dynamics and Earthquake Engineering, 31 (11), pp. 1452-1464.

Koumousis V.K.,Gantes C.J, Bouckovalas G.D., Dimou C.K., Lemonis M.E. (2002), "Thessaloniki - Skopje crude oil pipeline at fault crossings: verification case study", 4th Hellenic Conference on Metal Structures, Patra, 24-25 May (in Greek).

O'Rourke M.J, X. Liu (1999): "Response of buried pipelines subject to earthquake effects", Monograph Series, Multidisciplinary Center for Earthquake Engineering Research (MCEER).

Odina L. & Tan R. (2009), "Seismic fault displacement of buried pipelines using continuum finite element methods", Proceedings of the ASME 2009 28th international conference on ocean, offshore and arctic engineering, OMAE2009-79739. Honolulu, Hawaii.

Roudsari T.M., Seif M.A. & Jamshidi K.H. (2013), "Numerical Study of Pipe-Soil Interaction Subjected to Strike-Slip Faulting", ICPTT 2013, ASCE pp. 695-704.

Takada S., Liang J-W. & Li T. (1998), "Shell-Mode Response of Buried Pipelines to Large Fault Movements", Journal of Structural Engineering Vol. 44a (March 1998), JSCE, pp. 1637-1646.

Trifonov, O.V., Cherniy, V.P. (2010): "A semi-analytical approach to a nonlinear stress-strain analysis of buried steel pipelines crossing active faults", Soil Dynamics and Earthquake Engineering, 30 (11), pp. 1298-1308.

Trifonov, O.V., Cherniy, V.P. (2012): "Elastoplastic stress-strain analysis of buried steel pipelines subjected to fault displacements with account for service loads", Soil Dynamics and Earthquake Engineering, 33 (1), pp. 54-62.

Xie X., Symans M. D., O'Rourke M. J., Abdoun T. H., O'Rourke T. D., Palmer M. C. & Stewart H. E. (2011), "Numerical modeling of buried HDPE Pipelines subjected to strike-slip faulting", Journal of Earthquake Engineering 15, pp. 1273–1296.